Available online at www.eccomasproceedia.org
Eccomas Proceedia SMART (2023) 119-127

ECCOMAS
Proceedia

X ECCOMAS Thematic Conference on Smart Structures and Materials
SMART 2023
D.A. Saravanos, A. Benjeddou, N. Chrysochoidis and T. Theodosiou (Eds)

RESONANCE CAPTURE CASCADE IN A NONLINEAR PIEZOELECTRICAL SHUNT AND A VIBRATING FRAME

KEVIN DEKEMELE *, CHRISTOPHE GIRAUD-AUDINE† AND OLIVIER THOMAS‡

*Department of Electromechanical, Systems and Metal engineering
Ghent University, Technology park 125, 9052 Ghent, Belgium
e-mail: kevin.dekemele@ugent.be

† L2EP, Univ. Lille, Centrale Lille, Junia, HESAM Université, 8 Bd Louis XIV, 59000 Lille, France

‡ LISPEN, Arts et Métiers Institute of Technology, HESAM Université, 8 Bd Louis XIV, 59000 Lille, France

Abstract. In the last two decades, mechanical nonlinear vibration absorbers have been thoroughly investigated, in particular the nonlinear energy sink (NES). The NES has a variable natural frequency enabled by its nonlinear stiffness, typically a cubic hardening stiffness. This variable natural frequency increases the NES' bandwidth compared to linear alternatives and allows the NES to efficiently damp multi-frequency vibrations. Under transient conditions, resonance capture cascade (RCC) occurs, where several eigenfrequencies of a structure are sequentially dissipated from high to low frequency by the NES. Concurrent to the NES, piezoelectric vibration damping has also been actively researched, mainly focussing on linear techniques. In this work, it will be investigated numerically if RCC is possible in a nonlinear piezoelectric shunt. For this, piezoelectrical patches are bonded to a double frame structure that has two dominant eigenfrequencies. The investigated nonlinearity is a cubic voltage source proportional to the voltage over the piezoelectric patch's electrodes. This paper presents the theory and numerical evidence of RCC for the proposed circuit. As a perspective, the mechanical system and shunt from the numerical simulation are a proposal for a future proof of concept.

Key words: Vibration Control, Nonlinear Shunt, Resonance capture cascade

1 INTRODUCTION

To reduce high levels of undesirable vibrations in a mechanical structure, a linear spring-mass-damper system called a tuned-mass-damper (TMD) can be attached to the vibrating structure[1]. By designing the TMD's natural frequency to the frequency of vibration in the main structure, an efficient energy transfer is possible resulting in a high reduction of vibration. However, if the frequency of vibrations shifts or if the main structure vibrates with several frequencies at the same time, the performance of the TMD quickly deteriorates. To address these issues,

Peer-review under responsibility of the organizing committee of SMART 2023.
doi: 10.7712/150123.9770.437851

a vibration absorber with nonlinear forces, the nonlinear energy sink (NES), has been proposed [2]. The NES has a nonlinear hardening restoring force that implies a variable natural frequency, while the TMD has a fixed natural frequency. This enables a self-tuning property where the NES's natural frequency changes to match the vibrations of the main structure. If the main structure vibrates with more than one frequency induced by impulsive loads, the NES will self-tune towards the higher frequency first. When this mode is sufficiently reduced, the NES self-tunes itself to the second-to-highest frequency, and so on. This sequential self-tuning to vibration frequencies from high to low is called resonance capture cascade (RCC) [3, 4, 5]. Besides mechanical vibration control devices, mechanical vibrations can also be transferred and dissipated to the electrical domain through piezoelectrical transducers [6]. On the electrical side, a linear resonant shunt is typically used, with a tuning methodology similar to the mechanical TMDs [7]. Linear shunt circuits have the same drawbacks as linear TMDs. Piezoelectrical NESs have been proposed in [8] with a hardening charge-voltage relationship, which requires an enormous electric gain that leads to practical issues in the electronic circuit. To solve this issue, the nonlinear component in the shunt that will be used here depends on the piezoelectric voltage that is measured over the electrodes of the piezoelectric material. Such a component was first proposed in [9], which quadratically depends on the piezoelectric voltage, and later, where a cubic-hardening relation was used [10]. In particular, the existence of resonance capture cascade is investigated for this particular type of circuit. The paper is structured as follows: in the next section, the equations of motion are presented under impulsive load. Then, in section 3 harmonic balancing is applied to solve the nonlinear differential equations which yield a slow invariant manifold. A numerical example is presented in section 4 which validates the previously obtained slow invariant manifold. Finally, the conclusions are stated.

2 SYSTEM DESCRIPTION

The system under consideration is a linear mechanical system fitted with a piezoelectric patch (Figure 1), and is described by the following equations of motion:

$$\begin{aligned} &\ddot{q}_i + 2\zeta_i\hat{\omega}_i\dot{q}_i + \hat{\omega}_i^2 q + \frac{\theta_i}{m_i}V = 0 \quad \text{for } i \in [1,2,\ldots \text{n }], \\ &C_\text{p}V - Q - \sum_{r=1}^{n}\theta_r q_r = 0 \\ &V + L\ddot{Q} + R\dot{Q} + V_\text{nl} = 0 \end{aligned} \tag{1}$$

where the q_i are the modal displacements of the mechanical structure, $\hat{\omega}_i$ the i'th short circuit eigenfrequency, Q, V, C_p are the charge, the voltage and capacitance at the piezoelectric material's (PEM) electrodes, respectively, m_i, ζ_i and θ_i are the modal mass, the modal damping and the modal electromechanical coupling factor, respectively and L, R and V_nl are the shunt circuit's inductance, resistance and nonlinear component. The considered nonlinear component is proportional to the piezoelectric voltage cubed, $V_\text{nl} = \beta_c V^3$. Introducing a change of variables $\bar{q}_i = \sqrt{m_i}q_i$, $\bar{Q} = \sqrt{L}Q$ and $\bar{V} = V/\sqrt{L}$, then inserting the second equation in the third

with k_i the dimensionless modal electromechanical coupling factor, ω_e is the electrical eigenfrequency, r_i the ratio of the electrical and mechanical natural frequencies and ζ_e the electrical damping ratio.
In order to obtain the required inductor and nonlinearity, these impedances will be synthesized with active opamp circuits, as shown on Figure 2. The details of this circuit are found in [10].

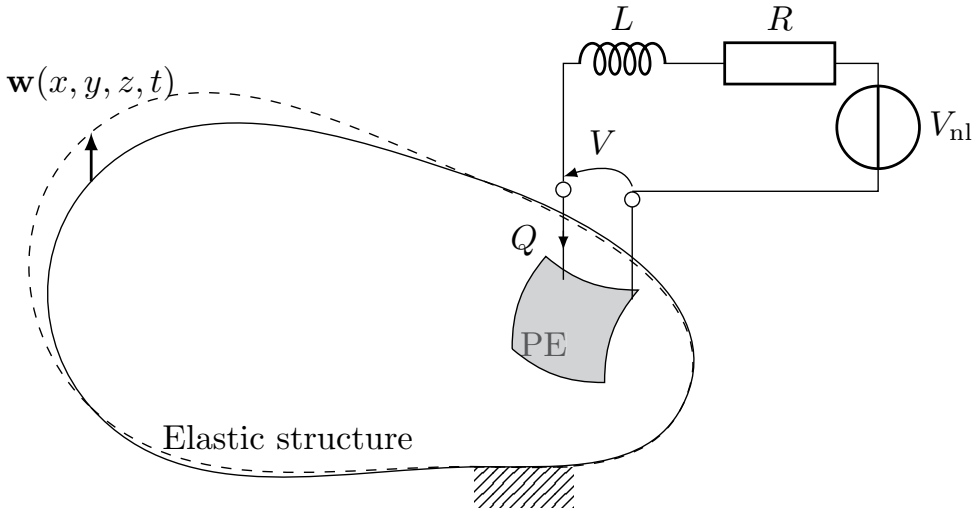

Figure 1: An elastic mechanical system with piezoelectric material (PE) that has a nonlinear shunt.

equation of (1) in order to describe the equations only in the dynamic variables $\bar{V}$ and $\bar{q}_i$ yields:

$$\begin{aligned} &\ddot{\bar{q}}_i + 2\zeta_i\hat{\omega}_i\dot{\bar{q}}_i + \hat{\omega}_i^2\bar{q} + \frac{k_i}{r_i}\bar{V} = 0 \quad \text{for } i \in [1,2,\dots \text{n }], \\ &\ddot{\bar{V}} - \omega_e\sum_{r=1}^{n}\omega_r k_r\ddot{\bar{q}} + 2\zeta_e\omega_e\left(\dot{\bar{V}} - \omega_e\sum_{r=1}^{n}\omega_r k_r\dot{\bar{q}}\right) + \omega_e^2\bar{V} + \gamma\omega_e^2\bar{V}^3 = 0 \end{aligned} \tag{2}$$

where

$$k_i^2 = \frac{\omega_i^2 - \hat{\omega}_i^2}{\omega_i^2} = \frac{\theta_i^2}{\omega_i^2 C_\mathrm{p} m_i}, \quad \omega_e^2 = \frac{1}{C_\mathrm{p}L}, \quad r_i = \frac{\omega_e}{\omega_i}, \quad \gamma = \beta_c L, \quad \zeta_e = \frac{R}{2}\sqrt{\frac{C_\mathrm{p}}{L}} \tag{3}$$

3 HARMONIC BALANCING AND SLOW INVARIANT MANIFOLD

The next steps in the procedure is to apply harmonic balancing in the modal eigenfrequencies of the mechanical system. To facilitate this, the following complex variables of Manevitch[11]

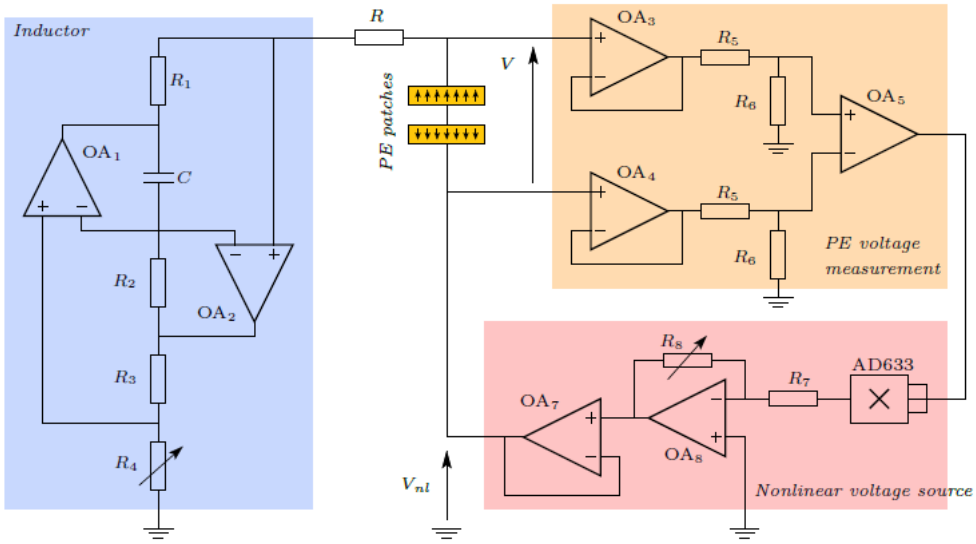

Figure 2: Circuit with synthetic inductor (left) and cubic voltage obtained from the multiplier circuit.

are defined:

$$2A_i(t)e^{j\omega_i t} = \bar{q}_i - j\dot{\bar{q}}_i/\omega_i \quad 2B_i(t)e^{j\omega_i t} = \bar{V}_i - j\dot{\bar{V}}_i/\omega_i \tag{4}$$

where the original variables are then substituted by:

$$\begin{aligned} &\bar{q}_i = A_i(t)e^{j\omega_i t} + A_i^*(t)e^{-j\omega_i t} \quad \dot{\bar{q}}_i = j\omega_i A_i(t)e^{j\omega_i t} - j\omega_i A_i^*(t)e^{-j\omega_i t} \\ &\text{for } i = 1, ..., n \\ &\bar{V} = \sum_{r=1}^{n} \underbrace{B_r(t)e^{j\omega_r t} + B_r^*(t)e^{-j\omega_r t}}_{\bar{V}_r} \quad \dot{\bar{V}} = \sum_{r=1}^{n} \underbrace{j\omega_r B_r(t)e^{j\omega_r t} - j\omega_r B_r^*(t)e^{-j\omega_r t}}_{\dot{\bar{V}}_i} \end{aligned} \tag{5}$$

where * stands for complex conjugate and $\bar{V}_r$ is the contribution of mode r to $\bar{V}$. Deriving (4) w.r.t. time yields, after some steps [12]:

$$\begin{aligned} &\ddot{q}_i + \omega_i^2 q_i = j2\omega_i \dot{A}_i e^{j\omega_i t} \\ &\ddot{\bar{V}}_i + \omega_i^2 \bar{V} = j2\omega_i \dot{B}_i e^{j\omega_i t}. \end{aligned} \tag{6}$$

The second derivative of the piezoelectric voltage is $\ddot{\bar{V}} = \sum_{r=1}^{n} \ddot{\bar{V}}_r$. Substituting (5) and (6) into (2) and results gives:

$$\begin{aligned} &j2\omega_i \dot{B}_i - \omega_i^2(1 - r_i^2)B_i + j2\zeta_e\omega_e\omega_i B_i + \gamma\omega_e^2 \left(-3B_i^2 B_i^* + 6B_i \sum_{r=1}^{n} B_r B_r^* \right) \\ &- k_i\omega_e\omega_i \left(j2\omega_i \dot{A}_i - \omega_i^2 A + j2\zeta_e\omega_i\omega_e k_i A \right) = 0 \end{aligned} \tag{7}$$

Applying a multiple time scales procedure to (7) allows to consider the slow dynamics. In the end, the procedure, detailed in [4, 12], results in an omission of the time derivatives. Finally, the complex variables are written in polar form, $A_i = \frac{a_i}{2}e^{j\alpha_i}$ and $B_i = \frac{b_i}{2}e^{j\beta_i}$ and a $2n$-dimensional slow invariant manifold (SIM) is found:

$$a_i^2\omega_i^4 r_i^2 k_i^2\left(4\zeta_e^2 r_i^2+1\right) = \left((2\zeta_e r_i)^2 + \left[(1-r_i^2) + r_i^2\gamma\left(\frac{3}{4}b_i^2 - \frac{3}{2}\sum_{r=1}^{n} b_r^2\right)\right]^2\right) b_i^2 \tag{8}$$

for $i \in$ [1,2, ... n],

This SIM reveals an interaction between modes, more specifically, a_i not only depends on b_i but also b_j, $j \neq i$. This modal interaction is not present in linear systems.

4 EXAMPLE SYSTEM

A numerical simulation will now prove the existence of RCC for the particular nonlinear circuit investigated here. The corresponding SIMs obtained from (8) are compared to the numerical simulations. To obtain two vibration modes, two frames with tip mass are connected together with a spring. Figure 3 is a scheme of this structure. The deflection of the beams $w_j(y,t)$ is an assumed mode according to the static deflection:

$$w_j(y,t) = \phi(y_j)r(t) = \frac{1}{2}\left(3\left(\frac{y_j}{L_b}\right)^2 - \left(\frac{y_j}{L_b}\right)^3\right) r(t) \tag{9}$$

Where $j = 1, 2$ stand for left and right beam, respectively. The tip displacements are $x_1(t) = w_1(L_b, t)$ and $x_2(t) = w_2(L_b, t)$. The equivalent mass and stiffness associated with the assumed mode is computed as follows, when assuming an Euler beam:

$$\begin{aligned} m_{j,eq} &= \rho_b A\int_0^{L_b}\phi^2(y_j)dy + 2\cdot\rho_p h_p b_p\int_{L_1}^{L_2}\phi^2(y_j)dy \\ k_{j,eq} &= Y_b I_b\int_0^{L_b}\left(\frac{\partial^2\phi(y_j)}{\partial y_j^2}\right)^2 dy \end{aligned} \tag{10}$$

This quasi-static approach allows the beams to be regarded as a spring and mass. Here, the tip mass is chosen to the be equal to the beam's total mass ($m_{bj} = m_{j,eq}$) and the connecting spring is equal to k_j. The dimensions and parameters on Table 1 allow to compute the coefficients of the equations of motion in $r_j(t)$, with the complete procedure found in [13]. Through modal decomposition of $r_1(t)$ and $r_2(t)$, (1) will be obtained. The modal parameters and the initial conditions for unity-mass eigenvectors are presented in Table 1 on the right, together with the nonlinear shunt under consideration. To simulate the an impulsive load on the system, the first tip mass is given an initial velocity s.t. $\dot{r}_1(0) = 0.1\ \mathrm{m/s}$ with the results shown in Figure 4 .

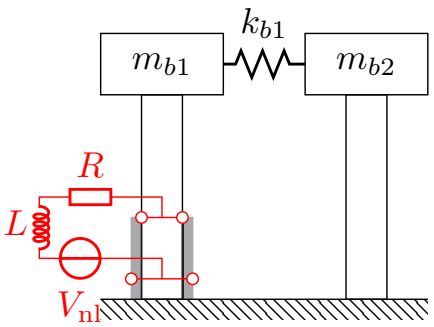

Figure 3: An elastic mechanical system with piezoelectric material (PE) that has a nonlinear shunt.

The tip mass vibrations in Figure 4a decays over about 2 seconds, where first the higher frequency is damped and then the lower frequency. This is more clear when observing the envelopes of the modes a_1 and a_2 in Figure 4c, where first a_2 is damped and then a_1. The electrode's voltage in Figure 4b and its corresponding wavelet transform, Figure 4d, shows the resonance capture cascade, i.e. the sequential transfer of vibration modes. The 4-dimensional SIM is compared to this simulation. In Figure 4e, the 4-dimensional SIM is projected on the $a_1 - b_1$ phase plane, for $a_2 = 5.3 \cdot 10^{-5}$ and $a_2 = 0$. Figure 4f is the SIM projected on the $a_2 - b_2$ phase plane for $a_1 = 8.1 \cdot 10^{-5}$ and $a_1 = 0$. The time simulations are also plot on these phase planes. The mechanism behind RCC is elucidated by the SIMS. For the non-zero a_2, the b_1 is small in the $a_1 - b_1$ plane , which explains the very slow decay of a_1 initially. as there is very little activity for this mode in the damping circuit. On the other SIM, b_2 remains large for nonzero a_1, and even the inefficient left part of the SIM is pushed down. This explains why a_2 is damped first. Once a_2 is sufficiently damped, the $a_1 - b_1$ SIM shifts to the right, increasing b_1 and initiating the efficient decay of a_1.

5 CONCLUSIONS

In this paper, the capabilities of a nonlinear shunt for resonance capture cascade (RCC) was investigated. The shunt had a cubic nonlinearity of the voltage over the electrodes of the piezo. By applying harmonic balancing, a multidimensional SIM was found that describes the relation between the vibration modes. The SIM hinted that vibration modes could interact with each other through the nonlinearity. Under shock load, this interaction led to RCC, where the vibrations in the main structure are damped sequentially per mode, in the order from high to low frequency. As a perspective, this will be experimentally tested on a vibrating frame having 2 vibration modes. The nonlinear shunt can be realized through multiplier circuits.

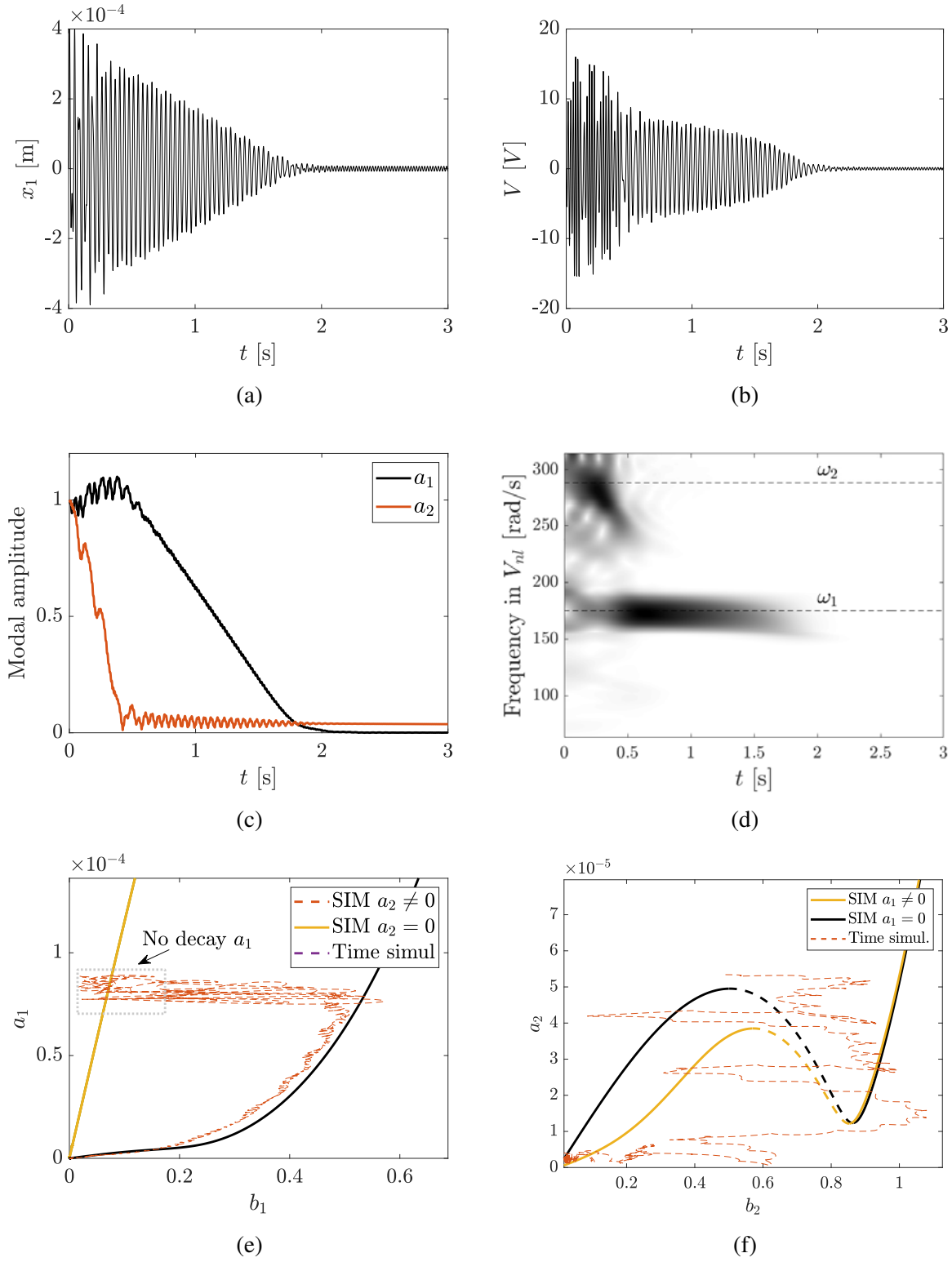

Figure 4: Simulation of system in Figure 3, (a) first beam tip displacement x_1, (b) the voltage over the piezoelectric material's electrodes, (c) the envelope of the vibration modes, (d) the wavelet transform of the voltage of (b), (e) $a_1 - b_1$ phase plot and (f) $a_2 - b_2$ phase plot.

Beam		
L_b [mm]	Length	166
b_b [mm]	Width	35
h_b [mm]	Thickness	0.2
Y_b [GPa]	Young's Modulus	72
ρ_b [kg/m^3]	Mass Density	2800
PE Mech.		
L_p [mm]	Length	50
b_p [mm]	Width	30
h_p [mm]	Thickness	0.02
$Y_1^{\mathbb{E}}$ [GPa]	Young's Modulus	62.2
ρ_p [kg/m^3]	Mass Density	7800
PE Elec.		
ϵ_T [nF/m]	Dielectric const.	1750
d_{31} [pC/N]	PE charge const.	-180

PEMS	
$\omega_{1,2}$ [rad/s]	175.1, 288.7
$\hat{\omega_{1,2}}$ [rad/s]	176.87, 289.9
$\theta_{1,2}$ [N/V]	0.0111, 0.0121
C_p [nF]	202
$k_{1,2}$ [-]	0.141, 0.094
$r_{1,2}$ [-]	0.951, 0.5774
$\zeta_{1,2}$ [-]	0, 0
$\dot{q}_{1,2}(0)$ [m/s]	-0.0142, -0.0154
Nonlinear shunt	
L [H]	178
R [Ω]	3430
β_c [1/V^2]	0.02

Table 1: Material constants for numerical simulations (left) and modal parameters and shunt parameters (right).

REFERENCES

[1] J. P. Den Hartog, *Mechanical vibrations*. Courier Corporation, 1985.

[2] A. F. Vakakis, "Inducing passive nonlinear energy sinks in vibrating systems," *J. Vib. Acoust.*, vol. 123, no. 3, pp. 324–332, 2001.

[3] K. Dekemele, R. De Keyser, and M. Loccufier, "Performance measures for targeted energy transfer and resonance capture cascading in nonlinear energy sinks," *Nonlinear Dynamics*, vol. 93, no. 2, pp. 259–284, 2018.

[4] G. Habib and F. Romeo, "Tracking modal interactions in nonlinear energy sink dynamics via high-dimensional invariant manifold," *Nonlinear Dynamics*, vol. 103, no. 4, pp. 3187–3208, 2021.

[5] K. Dekemele, P. Van Torre, and M. Loccufier, "Design, construction and experimental performance of a nonlinear energy sink in mitigating multi-modal vibrations," *Journal of Sound and Vibration*, vol. 473, p. 115243, 2020.

[6] N. W. Hagood and A. Von Flotow, "Damping of structural vibrations with piezoelectric materials and passive electrical networks," *Journal of sound and vibration*, vol. 146, no. 2, pp. 243–268, 1991.

[7] O. Thomas, J. Ducarne, and J.-F. Deü, "Performance of piezoelectric shunts for vibration reduction," *Smart Materials and Structures*, vol. 21, no. 1, p. 015008, 2011.

[8] T. M. Silva, M. A. Clementino, C. De Marqui Jr, and A. Erturk, "An experimentally validated piezoelectric nonlinear energy sink for wideband vibration attenuation," *Journal of Sound and Vibration*, vol. 437, pp. 68–78, 2018.

[9] Z. A. Shami, C. Giraud-Audine, and O. Thomas, "A nonlinear piezoelectric shunt absorber with a 2:1 internal resonance: Theory," *Mechanical Systems and Signal Processing*, vol. 170, p. 108768, 2022.

[10] ——, "Saturation correction for a piezoelectric shunt absorber based on 2: 1 internal resonance using a cubic nonlinearity," *Smart Materials and Structures*, 2023.

[11] L. Manevitch, "The description of localized normal modes in a chain of nonlinear coupled oscillators using complex variables," *Nonlinear Dynamics*, vol. 25, pp. 95–109, 2001.

[12] K. Dekemele, G. Habib, and M. Loccufier, "The periodically extended stiffness nonlinear energy sink," *Mechanical Systems and Signal Processing*, vol. 169, p. 108706, 2022.

[13] K. Dekemele, "Performance measures for nonlinear energy sinks in mitigating single and multi-mode vibrations: theory, simulation and implementation," Ph.D. dissertation, Ghent University, 2021.